Nigerian Research Journal of Engineering and Environmental Sciences 4(1) 2019 pp. 41-54

Nigerian Research Journal of Engineering and Environmental Sciences
Journal homepage: www.rjees.com

Original Research Article

A Study on an Underwater Toroidal Vessel with Circular Cross-Section

Enoma, N.
Department of Mechanical Engineering, University of Benin, Nigeria.
n.enoma@uniben.edu

ARTICLE INFORMATION

Article history:
Received 24 May, 2019
Revised 28 May, 2019
Accepted 03 June, 2019
Available online 30 June, 2019

Keywords:
Containment shell
Finite element analysis
Hydrostatic pressure
Shell analysis
Submerged toroidal vessel

ABSTRACT

Thin-shell structures find widespread application in underwater fields and are constructed to withstand environmental loads, including hydrodynamic loads. For circular toroidal vessels, which are a form of shells of revolution, the design analysis has mainly been centred on uniform hydrostatic pressure loading. This assumption is quite reasonable for vessels in deeper waters, but very conservative for hydrostatically loaded toroidal shells in shallow waters where the theoretical critical pressures are relatively higher, as demonstrated in this paper. Here, the linear theory of shells was employed for formulating the membrane-stress-state results and Abaqus finite element tool was used for the linear eigenvalue analysis. Important structural features of circular toroids under hydrostatic pressure which, of course, varies linearly with depth are reported based on linear-elastic material properties.

1. INTRODUCTION

Submerged shell structures are essentially subjected to floatation forces in the subsea environment. The study of circular toroidal shells under external hydrostatic pressure in consideration of hydrostatic effects which varies linearly across the depth of the shell is of relevance to submarines, especially in relatively shallow waters. Traditional treatment of these toroidal shell forms is mainly centred on the consideration of uniform pressure loading across the entire walls of the vessels (Błachut and Jaiswal 2000; Du *et al.,* 2015). Although there are also not very many studies that have been carried out on circular toroidal shells under uniform pressure, most of these studies have focused on statics and elastic buckling behaviour of the shells with little experimental data (Galletly and Błachut 1995; Enoma and Zingoni 2016). For large circular toroidal vessels in deeper waters, the assumption of constant uniform pressure across external walls of the shells is quite reasonable, but this is not very accurate for shells in relatively shallow waters. The studies by Błachut and his team showed through numerical studies that some toroidal shells are not very sensitive to initial geometric imperfections, and hence may serve as alternative configurations for some external pressure applications (Galletly and Błachut 1995; Błachut and Jaiswal 1998a, 2000). For the effective design of circular toroidal shell structures intended to operate in shallow waters, it is essential to properly understand their structural response to hydrostatic effects in the subsea environment.

Early investigations of toroidal shell forms were based on uniform pressure application in mind (Novozhilov 1970; Flügge 1973; Zingoni 1997). Unlike other geometrically smooth shells of revolution subjected to uniformly distributed loading over the surface of the shells, it was noticed that without additional bending, the membrane-hypothesis solution could not predict the state of stress and strain at the turning points of the toroidal shell where the curvature changes from positive to negative Gaussian curvature and vice versa. Various approaches have been applied to obtain the exact solution valid for the entire toroid and for all opening ration A/a (Jordan 1962; Sander and Liepins 1963; Steele 1965; Novozhilov 1970). Although the solution has proved to be very difficult, some useful insights to the behaviour and design procedures for circular toroidal shells under uniform pressure have been achieved. Membrane-solution results for the problem of hydrostatically loaded toroidal shells is presented in the present paper, by solving the governing equations of equilibrium of general shells of revolution under axisymmetric loading (Zingoni 1997) and a non-dimensional form of membrane resultant in the meridional direction. The Abaqus finite element code is then employed to conduct eigenvalue analyses of various circular toroidal shell geometries under hydrostatic pressure. Ratios of key parameters are adopted to cover a wider spectrum in the parametric study, and it is assumed that the circular toroidal shells are made from steel and that the shell wall thickness is constant throughout in all cases.

2. GEOMETRICAL AND LOADING PRELIMINARIES

Figure 1 depicts the geometrical parameters of a complete circular toroidal shell under external hydrostatic pressure. The orthogonal (ϕ, θ) system of coordinates was adopted, where ϕ is the angular coordinate measuring the angle from the upward direction of the axis of revolution of the toroid to the normal to the shell middle surface at any point *P* in question and θ is the angular coordinate along the hoop circle of revolution for the toroidal shell. In the Figure, *a* is the radius of the local circular cross-section, *t* is the wall thickness, A is the toroidal mean radius (the distance from the axis of rotation to the centre of the local circular cross-section), h_o is the distance between the surface of the liquid and the apex of the vessel; *H* is the overall height of the vessel. Hence $h=H+h_o$, and h_ϕ is the vertical distance measured from the apex of the vessel to any point P in the vessel. x is the horizontal distance measured from the local axis y-y to any point P in the vessel. It is positive for points at the outer regions, but negative for points at the inner regions of the vessel.

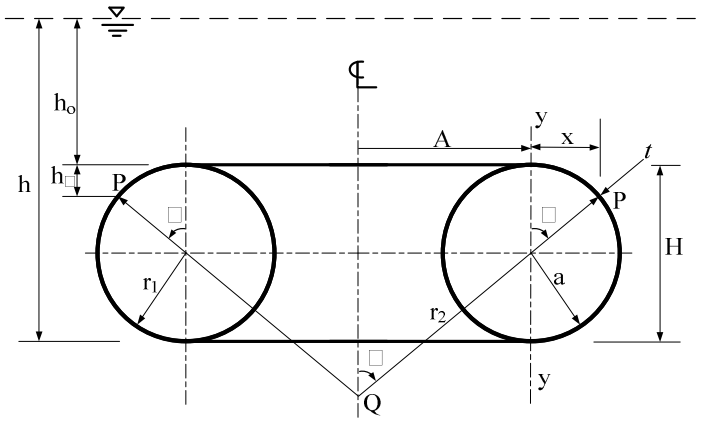

Figure 1: Geometry of a submerged circular toroidal shell

The response of shells of this type to external loading greatly depends on the adopted boundary conditions and support locations within the structures. The boundary conditions leading to the lowest load carrying capacity for toroidal shells under uniform external pressure have been presented through finite element analyses in Błachut and Jaiswal (1998b, 2000). Zingoni (1997) has shown analytically that bending disturbances at support regions will be minimal if the support is positioned in such a way that its reactions are tangential to the shell middle surface. However, should an occasion arise when this optimum support location/orientation is not adopted, Pavlovic and Papamakarios (1990) proposed that, the provision of full geometric constraints should be ensured at the support level of a spherical vessel as these turn out to be a much more efficient arrangement than that in which free movement and/or rotation are allowed to occur. Błachut and Jaiswal (1998a) however showed that critical buckling pressures for the over-restrained configurations of circular toroidal shells under uniform external pressure can be as much as about four times higher than the minimum buckling pressure.

It may therefore be assumed that the toroidal vessel under present consideration is supported at both the innermost and outermost equators simultaneously. The support reactions on the toroidal shell are also assumed to be uniformly distributed around supports circumference. The latter assumption is justified since where continuous supports at the inner and outer equators are not used, discrete supports are positioned close enough to evenly transfer reactions to the vessel so that the support conditions of the vessel are essentially axisymmetric. From the assumed support locations and definition of ϕ which indicates that two points are located on the middle surface of the toroidal shell for every value of ϕ, we may treat the circular toroidal shell as having four regions - the upper-outer ($0 \le \phi \le \pi/2$), lower-outer ($\pi/2 \le \phi \le \pi$), lower-inner ($0 \le \phi \le \pi/2$), and upper-inner ($\pi/2 \le \phi \le \pi$) regions - as shown in Figure 2.

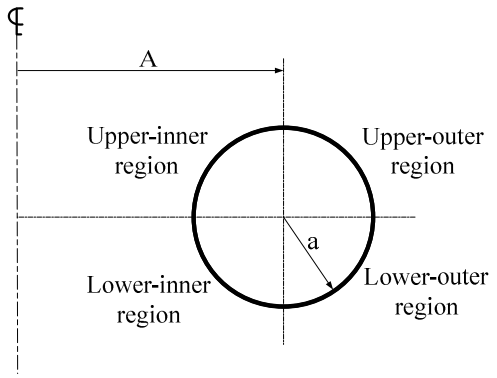

Figure 2: Regions of a circular toroidal shell

A point on the circular toroidal shell may also be characterized by the principal radii of curvature r_1 and r_2 of the shell middle surface in the meridional plane and the second principal plane, respectively. The first principal radius of curvature of the toroidal surface at any point P is the actual radius of curvature r_1 of the local circular meridional profile at that point, while the second principal radius of curvature r_2 is equal to the distance PQ (Figure 1), where Q is the point at which the surface normal at P intersects the axis of revolution of the toroidal shell. These can be expressed as:

$$r_1 = a, \text{ and } \quad r_2 = \frac{A+x}{\sin\phi} \tag{1}$$

where r_1 for the inner regions of the toroid being on the side of the shell surface opposite to that on which the axis of revolution lies, must be taken as negative.

The toroidal vessel under consideration is assumed to be completely submerged in a liquid of weight per unit volume (γ). The loading component per unit area of shell middle surface in the direction of the tangent to the shell meridian is zero (i.e. $p_\phi = 0$), since hydrostatic pressure acts purely perpendicular to the shell middle surface. The loading component per unit area of shell middle surface due to the hydrostatic loading from the external liquid may be expressed as:

$$p_r = \gamma\left(h_o + h_\phi\right) \tag{2}$$

This acts normal to the shell middle surface and it is considered positive if pointing away from the axis of revolution of the shell, while negative if pointing towards the axis of revolution of the shell. The maximum pressure (p_{max}) acting on the vessel is γh. This acts on the lowermost part of the vessel since hydrostatic pressure increases linearly with depth.

3. MEMBRANE SOLUTION

The membrane-hypothesis solution, which neglects flexural action is assumed to be, as a rule, a close approximation to the actual state of stress and deformation that occur within a shell (Pavlovic and Papamakarios 1990b; Zingoni and Pavlović 1993; Zingoni 2018). It may also serve as an approximate particular integral to the general bending-theory equations, to be added to the homogeneous solution of the equations. Such an approach is not pursued in this paper, but it will suffice to note at this juncture that the membrane solution provides a general idea about the structural response of shells such as the present one, where the concept of localized bending disturbance is applicable. In this Section, the membrane solution for a submerged circular toroidal shell is obtained by solving the governing equations of equilibrium of general shells of revolution under axisymmetric loading (Zingoni 1997). The solution is also presented in a parametric form.

3.1. Meridional Stress Resultant

The shell of revolution under present consideration is axisymmetrically loaded. The embrane- hypothesis assumes that an elemental part of the shell under the external loads p_ϕ and p_r may achieve force equilibrium through the action of in-plane stress resultants N_ϕ and N_θ alone. These stress resultants have been depicted in Figure 3, where $R = A + x$ is the radius of the circle of latitude of the toroidal shell element in question, (Figure 1), and all other terms are as previously defined.

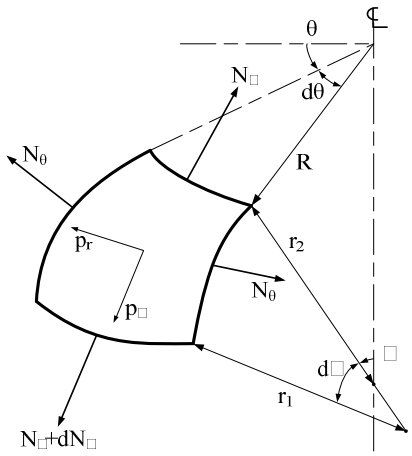

Figure 3: Element of an axisymmetrically loaded shell of revolution

For shells of revolution subjected to axisymmetric loading conditions, the general expression for the meridional stress resultant N_ϕ has been derived as (Flügge 1973, Zingoni 1997):

$$N_\phi = \frac{1}{r_2 \sin^2 \phi}\left[\int r_1 r_2 \left(p_r \cos\phi - p_\phi \sin\phi\right)\sin\phi d\phi\right] \tag{3}$$

Noting that $p_\phi = 0$ for all regions of the toroid, Equations (1) and (2) were used to eliminate r_1, r_2, p_θ, and p_ϕ from Equation (3) for each of the regions of the circular toroidal shell. The ensuing integral is then evaluated by applying the following boundary conditions. At the apex of the vessel (where, depending on the particular region under consideration, $\phi = 0$ and π for the upper outer region and upper inner region, respectively), N_ϕ must remain zero. Similarly, at the base of the vessel (where, depending on the particular region under consideration, $\phi = 0$ and π for the lower inner region and lower outer region, respectively), N_ϕ must be remain finite. The following meridional stress resultant N_ϕ may be obtained after some basic manipulations:

For the upper-outer region:

$$N_\phi = -\frac{a\gamma}{6\sin\phi(A + a\sin\phi)}\left[a^2(\cos\phi - 1)^2(2\cos\phi + 1) - 3aA\{\phi + \sin\phi(\cos\phi - 2)\}\right. \tag{4}$$
$$\left. + 3h_o \sin\phi(2A + a\sin\phi)\right]$$

For the lower-outer region:

$$N_\phi = -\frac{a\gamma}{6\sin\phi(A + a\sin\phi)}\left[a^2(2\cos^3\phi + 3\sin^2\phi + 2) - 3aA\{\phi - \pi + \sin\phi(\cos\phi - 2)\}\right. \tag{5}$$
$$\left. + 3h_o \sin\phi(2A + a\sin\phi)\right]$$

For the lower-inner region:

$$N_\phi = -\frac{a\gamma}{6\sin\phi(A-a\sin\phi)}\Big[a^2\left(2\cos^3\phi-3\sin^2\phi-2\right)+3aA\{\phi+\sin\phi(\cos\phi+2)\} - 3h_o\sin\phi(2A-a\sin\phi)\Big] \quad (6)$$

For the upper-inner region:

$$N_\phi = -\frac{a\gamma}{6\sin\phi(A-a\sin\phi)}\Big[a^2\left(2\cos^3\phi+3\cos^2\phi-1\right)+3aA\{\phi-\pi+\sin\phi(\cos\phi+2)\} - 3h_o\sin\phi(2A-a\sin\phi)\Big] \quad (7)$$

The last term (with h_o) in the bracket of each of Equations (4), (5), (6) and (7) is the contribution of the pressure loading from the liquid above the level of the submerged vessel. This contribution, which is constant for a particular depth, is a well-known solution for membrane resultant in meridional direction of uniformly pressurized toroidal shell (Flügge 1973; Zingoni 1997; Ventsel and Krauthammer 2001). The other terms in each of the expressions are contributions of the external hydrostatic effects from the top to bottom of the vessel. Hence, the above solution can also be applied to a toroidal vessel under combined internal vacuum (or uniform external pressure) and external hydrostatic loading from the top to bottom of the vessel.

3.2. Non-dimensional Meridional Results

Here, the distance between the surface of the liquid and the apex of the vessel is assumed to be zero (i.e $h_o = 0$), a non-dimensional parameter μ $(= A/a)$ (which will henceforth be referred to as the opening ratio of the toroidal vessel) is introduced to eliminate a and A from the right hand side of each of Equations (4), (5), (6) and (7) above. The following non-dimensional results for N_ϕ are obtained:

For the upper-outer region:

$$\frac{N_\phi}{A^2\gamma} = -\frac{1}{6\mu^2\sin\phi(\mu+\sin\phi)}\Big[(\cos\phi-1)^2(2\cos\phi+1)-3\mu\{\phi+\sin\phi(\cos\phi-2)\}\Big] \quad (8)$$

For the lower-outer region:

$$\frac{N_\phi}{A^2\gamma} = -\frac{1}{6\mu^2\sin\phi(\mu+\sin\phi)}\Big[\left(2\cos^3\phi+3\sin^2\phi+2\right)-3\mu\{\phi-\pi+\sin\phi(\cos\phi-2)\}\Big] \quad (9)$$

For the lower-inner region:

$$\frac{N_\phi}{A^2\gamma} = -\frac{1}{6\mu^2\sin\phi(\mu-\sin\phi)}\Big[\left(2\cos^3\phi-3\sin^2\phi-2\right)+3\mu\{\phi+\sin\phi(\cos\phi+2)\}\Big] \quad (10)$$

For the upper-inner region:

$$\frac{N_\phi}{A^2\gamma} = -\frac{1}{6\mu^2 \sin\phi(\mu - \sin\phi)}\left[\left(2\cos^3\phi + 3\cos^2\phi - 1\right) + 3\mu\{\phi - \pi + \sin\phi(\cos\phi + 2)\}\right] \quad (11)$$

It is observed from Equations (8), (9), (10) and (11) that the stress resultant N_ϕ in any of the regions of the vessel is directly proportional to A^2 (or to a^2, since a is proportional to A). For each of the toroidal regions, the non-dimensional stress variations $N_\phi / A^2\gamma$ are plotted against ϕ_c for μ (= 1.5, 3.0, and 6.0) as shown in Figure 4. ϕ_c in the Figure is defined as the angular coordinate along the circular meridian (measured from the local vertical axis of the circular cross-section towards the outer surface the toroid, round the circular meridian). Hence, ϕ_c is equal to ϕ at the outer regions of the vessel, while it is equal to $\phi + 180^o$ at the inner regions of the vessel. No values are presented for the zones near the turning points of the toroid as the adopted membrane hypothesis for shells of revolution results in some singularities at these locations.

3.3. Hoop Stress Resultant and Lateral Displacement

For each of the regions of the vessel, the membrane stress resultants in the hoop direction (N_θ) and the horizontal displacement (δ) may be obtained from (Zingoni 1997) as follows:

$$N_\theta = r_2\left(p_r - \frac{N_\phi}{r_1}\right) \quad (12)$$

$$\delta = \frac{1}{Et}(r_2 \sin\phi)\left(N_\theta - \nu N_\phi\right) \quad (13)$$

where E is the young's modulus of elasticity of the shell material, ν is the Poisson's ratio and all other terms are as previously defined. δ is considered positive when away from the axis of revolution, and the membrane stress resultants N_ϕ and N_θ are forces per unit length of the respective edge of a shell element, considered positive when tensile. The actual membrane stresses (σ_ϕ^m and σ_θ^m) in the meridional and hoop directions, respectively, can be obtained from Equations 14 and 15:

$$\sigma_\phi^m = \frac{N_\phi}{t} \quad (14)$$

$$\sigma_\theta^m = \frac{N_\theta}{t} \quad (15)$$

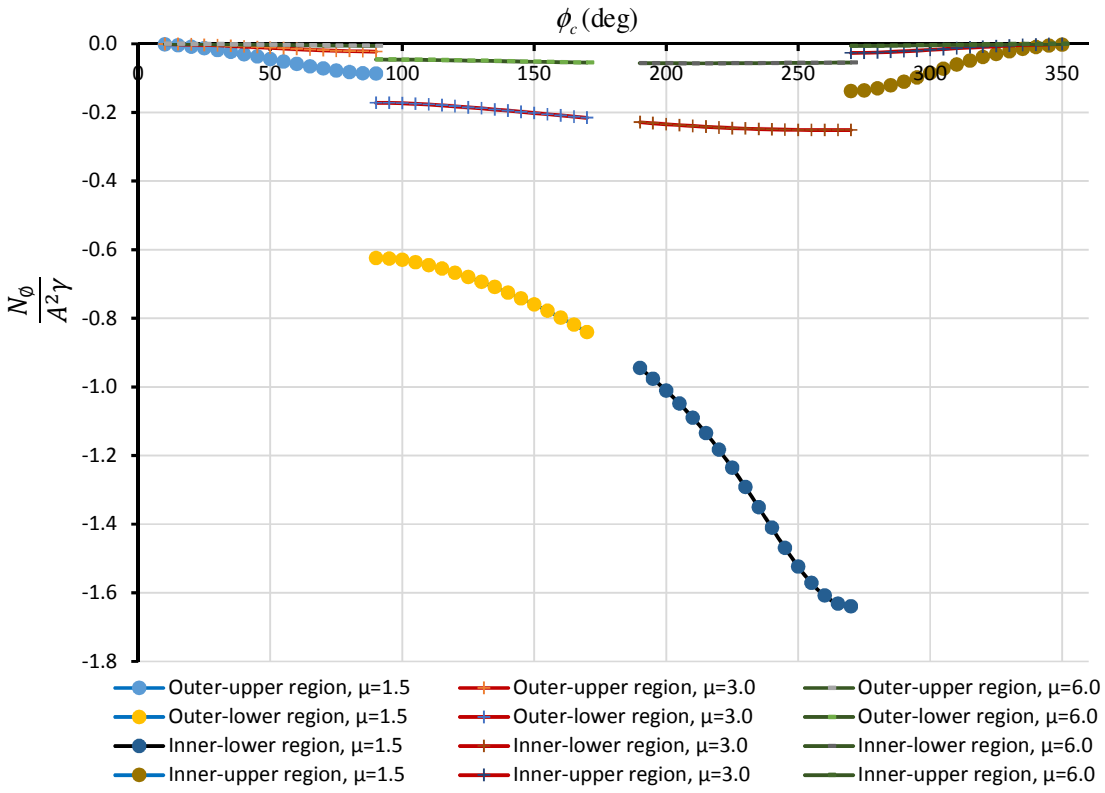

Figure 4: Non-dimensional meridional stress variations for the circular toroid under hydrostatic loading

As far as membrane results are concerned, it is noted from Figure 4 that, for each of μ considered, the parametric results of the meridional stress resultant gradually increases in compression from zero at the apex of the vessel, as expected. The degree of increase is dependent on the value of μ. As the toroidal opening ratio increases, it is observed, generally, that the value of meridional stress resultant within a toroidal shell reduces in compression. This is also the case with the degree of discontinuity in the meridional stress resultant in moving across the support junctions at both the inner and outer regions of the toroidal shell. The discontinuity in the meridional stress resultant, for all cases considered, are higher at the inner region compared to the outer region of the toroid. The meridional stress resultants are compressive throughout the toroidal shells as expected for external hydrostatic pressure loading condition.

It evident that membrane solution alone is not sufficient in providing complete information regarding the structural response of this shell type to hydrostatic pressure which, of course, varies linearly with depth. Due to localized bending, the solution entirely breaks down at the locations surrounding the supports and turning points (where the curvature changes from positive to negative Gaussian curvature), owing to the vanishing of the curvature $1/r_2$ there, as r_2 jumps from $+\infty$ (just within the outer surface) to $-\infty$ (just within the inner surface). It is also noticed that as a or A is increased, the mismatch in lateral displacement δ between adjacent regions of the vessel at the support junction reduces, and Figure 4 also indicates the likelihood of occurrence of meridional buckling of the toroidal vessel subjected to external hydrostatic loading. It is, therefore, important to provide some insight into the buckling performance of this shell form. The finite

element method has been found to permit a rapid and efficient analysis and design of shell structures in question, even of more complex and specialized studies. The Abaqus finite element code is employed next for the elastic buckling analyses of perfect circular toroids of different geometries subjected to hydrostatic pressure. For limiting cases, we compared our results with analytical and computational results in the literature.

4. BUCKLING OF SUBMERGED CIRCULAR TOROIDS

For the present problem, the Abaqus finite element code was used to estimate the first mode of buckling. The toroidal shells were modelled using both four-node doubly curved thin shell element with reduced integration (S4R) and three-node quadratic axisymmetric thin shell element with two integration points (SAX2) that are available in the program. These shell elements have been proven to be very effective in both static and buckling analyses (Błachut and Jaiswal 2000; Zingoni *et al.,* 2015). In the analysis, the program considers finite deflections and moderate rotations when formulating the stress/buckling problem. In Abaqus, integrations are performed in a plane for SAX2, hence the required results were computed in a shorter computer time compared to S4R. But the first buckling mode shape is not always symmetrical about the axis of revolution of the toroid, it varies for different boundary conditions and geometric parameters, hence S4R model was used as a check.

4.1. Basic Assumptions

The linear buckling analysis was carried out on the basis of some assumptions. Firstly, as already indicated in Section 2, the toroidal vessel was assumed to be constrained at the outermost and innermost equators simultaneously and the support condition of the vessel was assumed to be essentially axisymmetric. Secondly, external hydrostatic pressure P_r $(=\gamma h)$ is the essential loading on the shell and hence was assumed to be the only loading condition. This loading effect become more significant as the relative height of the vessel to the total depth of the external medium increases. Other loading conditions, including the net weight of the vessel material, are not considered. Finally, the vessels were assumed to be geometrically perfect and made from steel of constant wall thickness t, for which the Young's modulus E=210 *GPa* and the Poisson's ratio v=0.3.

4.2. Parametric Results

The elastic buckling behaviour of various circular toroidal geometries under hydrostatic pressure was studied. We started by investigating the effect of boundary conditions on the first buckling pressure and mode of submerged circular toroids. This was to identify the boundary conditions leading to the lowest buckling strength. We studied a couple of possible support conditions and presented only two sets of configurations - leading to the lowest and highest critical buckling loads, in that order - in Figure 5. Each of the shells has the following geometrical parameters: a=10, $\mu = 2$, $a/t = 100$, $h/H = 1$. The first shell which was supported with the set of configuration: $x \neq 0$, $y \neq 0$, $z = 0$, $\Phi_x \neq 0$, $\Phi_y \neq 0$, $\Phi_z \neq 0$ at the inner equator and $x = 0$, $y \neq 0$, $z \neq 0$, $\Phi_x \neq 0$, $\Phi_y \neq 0$, $\Phi_z \neq 0$ at the outer equator lost its stability through static bifurcation at $p_{cr} = 0.56MPa$ (Figure 5a), while the second shell which was fully fixed at both the inner equator and outer equator lost its stability through static bifurcation at $p_{cr} = 2.12MPa$ (Figure 5b). This shows that, depending on the support condition, the lowest critical buckling strength of a submerged toroidal shell could be up to one-fourth of the highest buckling load.

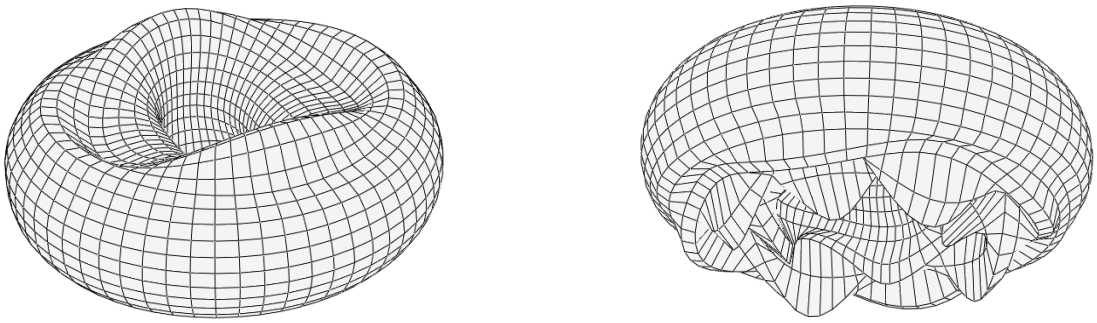

(a) First set (b) Second set

Figure 5: First buckling modes for various boundary conditions ($\mu = 2$, $a/t = 100$, $h/H = 1$)

It was observed that the lowest buckling strength is obtained from the first set of configuration, and the first buckling mode shape, as earlier indicated, also depends on geometric parameters and support conditions. For some configurations (e.g. $x \neq 0$, $y \neq 0$, $z = 0$, $\Phi_x = 0$, $\Phi_y = 0$, $\Phi_z = 0$ at the inner equator and $x = 0$, $y \neq 0$, $z \neq 0$, $\Phi_x = 0$, $\Phi_y = 0$, $\Phi_z = 0$ at the outer equator), the first buckling mode shape was found to be symmetrical about the axis of revolution of the toroidal shell (Figure 5). Hence, the number of waves n in the circumferential direction θ is zero (i.e. axisymmetric buckling mode). The buckling modes about the equatorial plane of hydrostatically loaded toroidal shells were found to be mainly antisymmetric for all cases. A typical example of an antisymmetric buckling mode about equatorial plane, including a section through the toroidal vessel is shown in Figure 6.

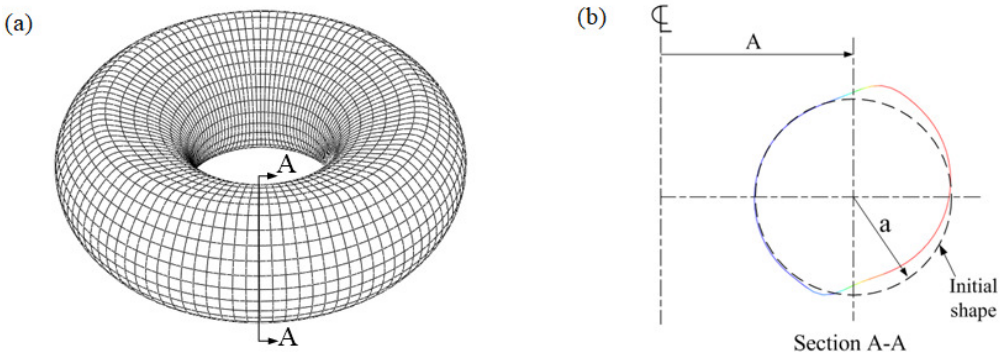

Figure 6: View of axisymmetric bifurcation buckling mode for a circular toroid under hydrostatic pressure ($n = 0, \mu = 2$, $a/t = 100$, $h/H = 1$): (a) the model, and (b) right-hand cross-section

Adopting the first set of boundary condition, a series of elastic bifurcation buckling pressure calculations was carried out for different μ ratios and for a single h/H ratio of 1. These were repeated for a single h/H ratio of 100. A constant a/t ratio of 20 was used for both cases. The variations of the elastic bifurcation buckling pressures for the two cases are shown in Figure 7. The curves are typical of the curves obtained by Błachut and Jaiswal (2000) for uniformly pressurized toroidal shells of circular cross-sections. It is seen from Figure 7 that the bifurcation pressures for the case of $h/H = 1$, for all μ ratios studied, are generally higher than those for $h/H = 100$. Noting that μ ratios of all the circular toroidal shells studied

are greater than 1, higher values of bifurcation buckling pressures are seen for smaller values of μ. This indicates that, depending on the material yield point, the bifurcation failure will likely govern the failure mode of circular toroidal shells with high μ ratios. Thus, circular toroidal geometries under external hydrostatic pressure with small μ ratios will likely fail by plastic collapse.

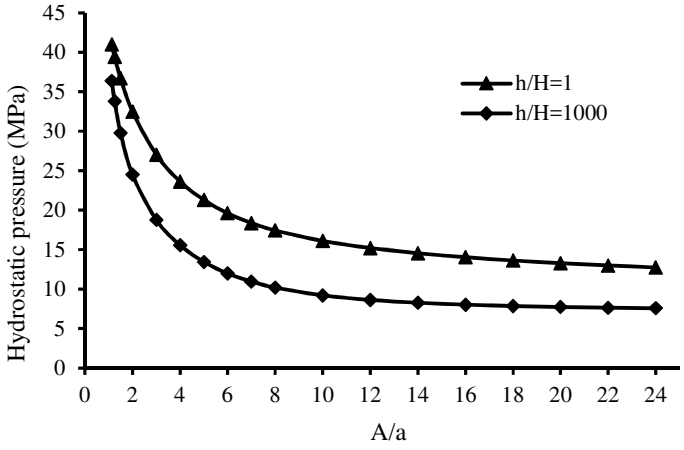

Figure 7: Bifurcation buckling pressures versus A/a ratio for circular toroidal shells with a/t=20

The effects of various shell thickness ratios a/t and toroidal opening ratios μ for different h/H ratios on the elastic bifurcation buckling pressure of hydrostatically loaded circular toroidal shells were also investigated. The elastic bifurcation buckling pressures obtained from the eigenvalue analyses are shown in Table 1. The results appear in a tabular instead of a graphical form to allow the presentation of the variation of the different non-dimensional parameters in the most concise manner.

For all cases considered, it is seen from Table 1 that there is a general decrease in the elastic bifurcation buckling pressure of a circular toroidal shell as the h/H ratio increases. That is as the water becomes shallower, the buckling pressure of a toroidal vessel increases. A general trend is also observed for the variations in the toroidal opening ratio μ: the buckling pressure decreases as μ increases. This make sense, since the tighter the torus (a μ value approaching 1.0), the stiffer it becomes, and hence the higher the buckling pressure. On the other extreme, as μ tends towards infinity (larger value of A), the effects of toroidal curvature become weaker, and the results for the toroidal shell will tend towards those for a long cylindrical shell. A similar trend is seen in the buckling pressures for toroidal vessels of different shell thickness ratios a/t - keeping all other parameters constant and increasing the shell thickness t of a circular toroidal vessel under hydrostatic loading, the buckling pressure of the vessel increases as expected. One can, therefore, conclude that the hydrostatic buckling pressure of a circular toroidal vessel will decrease if the toroidal opening ratio μ, or shallowness ratio of water h/H, or shell thickness ratio a/t increases.

Table 1: Comparison of bifurcation pressures for different h/H, μ, and a/t ratios of perfect circular toroidal shells under hydrostatic loading

		p_{cr} (MPa)				
a/t	h/H / μ	1	10	100	500	1000
20	1.25	39.452	35.521	33.952	33.810	33.792
	2.00	32.495	25.832	24.640	24.535	24.522
	4.00	23.646	16.451	15.654	15.586	15.577
	10.00	16.120	9.767	9.278	9.237	9.232
	20.00	13.300	8.208	7.799	7.764	7.760
100	1.25	0.6478	0.7799	0.7504	0.7474	0.7470
	2.00	0.5572	0.5706	0.5470	0.5448	0.5445
	4.00	0.4208	0.3629	0.3469	0.3455	0.3453
	10.00	0.2729	0.2025	0.1931	0.1923	0.1921
	20.00	0.1930	0.1310	0.1246	0.1241	0.1240
500	1.25	0.01008	0.01758	0.01717	0.01710	0.01709
	2.00	0.00898	0.01295	0.01254	0.01249	0.01248
	4.00	0.00711	0.00823	0.00792	0.00789	0.00788
	10.00	0.00484	0.00453	0.00434	0.00432	0.00432
	20.00	0.00349	0.00289	0.00277	0.00275	0.00275

4.3. Validation

The idealization employed in the Abaqus finite element software for the eigenvalue study and the results obtained were validated with analytical and computational results for uniformly pressurized circular toroidal vessels in the literature. The same idealization was used but the loading was changed from hydrostatic to uniform external pressure. The obtained elastic bifurcation buckling pressure results for a set of geometrical parameters are shown in the last column of Table 2. For ease of comparison, the parameters for the toroidal vessels analysed are as in Galletly and Błachut (1995) where the buckling pressures were calculated using the French finite element program, INCA. The results were compared with results from the studies by Sobel and Flügge (1967), Wang and Zhang (1991), and Galletly and Błachut (1995).

From Table 2, it seen that the obtained numerical results in the last column are almost identical to the results obtained from the French finite element program, INCA by Galletly and Błachut, and also compare very well with the results from the studies by Sobel and Flügge; and Wang and Zhang.

Table 2: Comparison of critical buckling pressures for perfect circular toroidal shells under uniform external pressure

		p_{cr} (MPa)			
a/t	μ	(Sobel and Flügge 1967)	(Wang and Zhang 1991)	Galletly and Błachut (1995)	Abaqus (SAX2) Present study
100	2.0	0.563	0.563	0.545	0.544
100	8.0	0.239	0.222	0.221	0.221
500	2.0	0.0126	0.0128	0.0125	0.0125
500	8.0	0.0052	0.005	0.005	0.00499

It was also observed that the critical buckling pressures computed using the well-known simple algebraic Equation (16), proposed by Jordan (1973) for an externally pressurized circular toroidal shell are in accordance with the results in the last column of Table 2. The achieved excellence agreement between the

results obtained from this study and the results from the literature leads us to conclude that the adopted idealization for the elastic buckling analysis of circular toroidal vessels under hydrostatic pressure in the Abaqus finite element program is a very accurate.

$$p_{cr} = 0.185E\left(\frac{t}{a}\right)^{7/3}\left(\frac{1}{\mu}\right)^{2/3} \tag{16}$$

The accuracy of the method is further seen in the last column of Table 1 where $h/H = 1000$, the critical hydrostatic pressures are almost the same with identical toroids under uniform external pressure in Table 2. This is expected for a limiting case, where the ratio h/H becomes very large, the critical buckling pressure of hydrostatically loaded circular toroid should approach that of a uniformly pressurized circular toroid with the same geometrical properties. Because, as h/H become very large, the linear load variation with depth of the external hydrostatic pressure on the vessel becomes insignificant. Hence, at this depth, the walls of the toroidal vessel will feel the external hydrostatic pressure like a uniform pressure loading. Thus, the adoption of the uniformly pressurized toroidal shell buckling solution for hydrostatically loaded toroidal shells in deeper waters is quite reasonable, but this would be very conservative for shallow water conditions where the theoretical critical pressures, are relatively higher.

5. CONCLUSION

This paper studied the structural behaviour of perfect circular toroidal vessels under external hydrostatic pressure loading which, of course, varies linearly across the height of the vessel. Firstly, the membrane-solution results were provided for the vessel. This solution facilitates the determination of membrane stresses and deformations that occur within the loaded vessel. Although the membrane solution fails at the support locations and turning points of the toroid (as expected, based on the adopted assumptions), it provides a useful approximation to the actual state of stress in the interior regions of the vessel. The membrane stress resultant in the meridional direction was also presented in a non-dimensional form. It was observed that the value of meridional stress resultant (which was compressive throughout the toroidal shell), reduces as the toroidal opening ratio μ increases. In the second part of the paper, Abaqus finite element code was employed for the eigenvalue analyses of various circular toroidal shell geometries. Ratios of key parameters were abducted to cover a wider spectrum in the parametric study which, generally, indicated that the critical buckling pressure of a circular toroidal vessel under hydrostatic pressure will decrease if the toroidal opening ratio μ, or shallowness ratio of water *h/H*, or shell thickness ratio *a/t* is increased. It was also found that the calculated bifurcation pressures for circular toroidal vessels under hydrostatic pressures at higher values of *h/H* became almost identical with those of toroidal vessels with the same geometries but under uniform pressure. This led to the conclusion that the traditional adoption of the uniformly pressurized toroidal shell buckling solution is quite reasonable for hydrostatically loaded toroidal shells in deeper waters, but very conservative for shells in shallow waters where the theoretical critical pressures are relatively higher. Hence, the inclusion of hydrostatic effects in the estimation of critical buckling pressures of circular toroidal vessels under hydrostatic loading is recommended, more so, for shallow waters.

6. CONFLICT OF INTEREST

There is no conflict of interest associated with this work.

REFERENCES

Błachut, J. and Jaiswal, O.R. (1998a). Buckling under external pressure of closed toroids with circular and elliptical cross sections. *In*: B.H. Topping, ed. *Advances in civil and structural engineering computing for practice*. Edinburgh: Civil- Comp Press, pp. 323–334.

Błachut, J. and Jaiswal, O.R. (1998b). Buckling of imperfect ellipsoids and closed toroids subjected to external pressure. *ASME PVP*, 368, pp. 121–128.

Błachut, J. and Jaiswal, O.R. (2000). On buckling of toroidal shells under external pressure. *Computers & Structures*, 77, pp. 233–251.

Du, Q., Cui, W. and Zhang, B. (2015). Buckling characteristics of a circular toroidal shell with stiffened ribs. *Ocean Engineering*, 108, pp. 325–335.

Enoma, N. and Zingoni, A. (2016). On the feasibility of the parabolic ogival cross-section for liquid-filled toroidal vessels. *In*: A. Zingoni, (ed). *Insights and Innovations in Structural Engineering, Mechanics and Computation. Proceedings of the Sixth International Conference on Structural Engineering, Mechanics and Computation, 5-7 September 2016, Cape Town, South Africa.* Cape Town: Taylor & Francis Group, pp. 793–798.

Flügge, W. (1973). *Stresses in shells*. Berlin: Springer-Verlag.

Galletly, G.D. and Błachut, J. (1995). Stability of complete circular and non-circular toroidal shells. *Proceedings of the Institution of Mechanical Engineers: Journal of Mechanical Engineering Science*, 209, pp. 245–255.

Jordan, P.F. (1962). Stresses and deformations of the thin-walled pressurized torus. *The Aerospace Sciences*, 29, pp. 213–225.

Jordan, P.F. (1973). Buckling of toroidal shells under hydrostatic pressure. *AIAA*, 11 (10), pp. 1439–1441.

Novozhilov, V. V. (1970). *Thin elastic shells*. Groningen: Wolters-Noordhoff.

Pavlovic, M.N. and Papamakarios, A. (1990a). The structural behaviour of liquid-filled spherical vessels. Part 2: parametric study and examples. *Thin-Walled Structures*, 10, pp. 329–354.

Pavlovic, M.N. and Papamakarios, A. (1990b). The structural behaviour of liquid-filled spherical vessels. Part 1: Background and theoretical preliminaries. *Thin-Walled Structures*, 10, pp. 195–214.

Sander, J.L. and Liepins, A.A. (1963). Toroidal membrane under internal pressure. *AIAA*, 1 (9), pp. 2105–2110.

Sobel, L.H. and Flügge, W. (1967). Stability of toroidal shells under uniform external pressure. *AIAA*, 5 (3), pp. 425–431.

Steele, C.R. (1965). Toroidal pressure vessels. *Journal of Spacecraft and Rockets*, 2, pp. 937–943.

Ventsel, E. and Krauthammer, T. (2001). *Thin plates and shells: theory, analysis, and applications*. New York: Marcel Dekker, Inc.

Wang, A. and Zhang, W. (1991). Asymptotic solution for buckling of toroidal shells. *International Journal of Pressure Vessels and Piping*, 45 (1), pp. 61–72.

Zingoni, A. (1997). *Shell structures in civil and mechanical engineering*. London: Thomas Telford Publishing.

Zingoni, A. (2018). *Shell structures in Civil and Mechanical engineering: Theory and Analysis (Second Edition)*. London: ICE Publishing.

Zingoni, A., Enoma, N., and Govender, N. (2015). Equatorial bending of an elliptic toroidal shell. *Thin-Walled Structures*, 96, pp. 286–294.

Zingoni, A. and Pavlović, M.N. (1993). A note on the accuracy of the Geckeler approximation. *Engineering Computations: International Journal for Computer-Aided Engineering and Software*, 10 (4), pp. 369–379.